Chinese Journal of Aeronautics 25 (2012) 691-697

Contents lists available at ScienceDirect

Chinese Journal of Aeronautics

journal homepage: www.elsevier.com/locate/cja

Energy Conversion Efficiency of Rainbow Shape Piezoelectric Transducer

LIU Xiangjian, CHEN Renwen*, ZHU Liya

Aeronautical Science Key Laboratory for Smart Materials and Structures, Nanjing University of Aeronautics and Astronautics, Nanjing 210016, China

Received 20 June 2011; revised 20 September 2011; accepted 19 October 2011

Abstract

With the aim to enhance the energy conversion efficiency of the rainbow shape piezoelectric transducer, an analysis model of energy conversion efficiency is established based on the elastic mechanics theory and piezoelectricity theory. It can be found that the energy conversion efficiency of the rainbow shape piezoelectric transducer mainly depends on its shape parameters and material properties from the analysis model. Simulation results show that there is an optimal length ratio to generate maximum energy conversion efficiency and the optimal length ratios and energy conversion efficiencies of beryllium bronze substrate transducer and steel substrate transducer are (0.65, 2.21%) and (0.65, 1.64%) respectively. The optimal thickness ratios and energy conversion efficiencies of beryllium bronze substrate transducer and steel substrate transducer are (1.16, 2.56%) and (1.49, 1.57%) respectively. With the increase of width ratio and initial curvature radius, both the energy conversion efficiencies decrease. Moreover, beryllium bronze flexible substrate transducer is superior to the steel flexible substrate transducer.

Keywords: energy conversion efficiency; rainbow shape; piezoelectric transducer; theoretical analysis; energy harvesting; electromechanical coupling coefficient

1. Introduction

The use of microelectronic devices has grown steadily in the past few decades. It is a challenge to provide efficient and clean power for these devices. In most cases, these devices have all relied on the use of electrochemical batteries for providing electrical energy to work. However, the increase in power used by the electronics has led to a reduction in battery lifespan and has limited the functionality of the devices. In order to extend the life, researchers have begun exploring methods of obtaining electrical energy from the ambient energy surrounding the devices. Potential energy sources are available in the operating environment of microdevices include solar, thermal, acoustic vibrations, electrical, or some combination thereof. Because of the widespread and high energy density [1], more and more researchers are interested in harvesting ambient vibration energy.

After reviewing and making a comparison of methods of scavenging vibration energy, Roundy, et al. [2-3] have concluded that piezoelectric harvesters [4-13] scavenging ambient vibration energy are very promising, because the piezoelectric harvesters have significantly higher efficiency than other potential power scavenging technologies, such as electrostatic harvesters [14], electromagnetic harvesters [15], etc. Furthermore, the piezoelectric harvesters require no external voltage source and are particularly attractive for use in micro-electro-mechanical systems (MEMS). As a result, piezoelectric materials for scavenging energy from ambient vibration sources have recently seen a dramatic rise in the use for energy harvesting. This

*Corresponding author. Tel.: +86-25-84893466-185.
E-mail address: rwchen@nuaa.eud.cn
Foundation items: National Natural Science Foundation of China (10972102); Research Fund for the Doctoral Program of Higher Education of China (200802870007); Technology Research and Development Program of Jiangsu Province (BE2009163)

doi:10.1016/S1000-9361(11)60435-4

includes the use of resonant piezoelectric-based structures of cantilever beam configuration. Other harvesting schemes [16-18] include the use of long strips of piezoelectric polymers in ocean or river-water flows, piez oelectric 'cymbal' transducers, piezoelectric 'drum' transducers, and piezoelectric windmill for generating electric energy from wind energy. However, these piezoelectric devices can only harvest the vibration energy of one direction and they have low efficiency in the surroundings with random vibration. With the aim to harvest multi-direction ambient vibration energy, a novel multi-direction ambient vibration energy harvester is proposed and a novel rainbow shape piezoelectric transducer is applied to the multi-direction vibration energy harvester [19]. Liu and Chen [19] have studied the feasibility of the rainbow shape piezoelectric transducer to harvest vibration energy. With the aim to enhance the generated electric energy, the energy conversion efficiency of the rainbow shape piezoelectric transducer should be studied.

In this paper, a method is presented to estimate the energy conversion efficiency of the rainbow shape piezoelectric transducer. Moreover, the numerical simulation is performed to analyze the influence of the shape parameters and material properties of the rainbow shape piezoelectric transducer on energy conversion efficiency.

2. Structure and Principle of Rainbow Shape Piezoelectric Transducer

Figure 1 shows the schematic diagram of the rainbow shape piezoelectric transducer consisting of a metal flexible substrate, two piezoelectric films and four electrodes. The metal flexible substrate sandwiched between two piezoelectric films and the piezoelectric film sandwiched between two electrodes. In Fig. 1, b_p, l_p and t_p are the width, length and thickness of the piezoelectric film respectively; b_m, l_m and t_m the width, length and thickness of the metal flexible substrate respectively; and R is the initial curvature radius of the transducer.

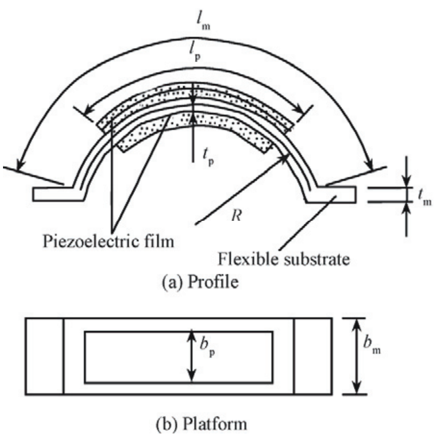

Fig. 1 Sketch map of rainbow shape piezoelectric transducer.

The rainbow shape piezoelectric transducer can be deformated as the external force applied to the transducer. So the strain and stress of the piezoelectric films change at the same time. According to the piezoelectricity theory, electric charge can be generated on the surface of the piezoelectric films as the strain and stress change. The linear constitutive equations that describe the mechanical and electrical behavior of piezoelectric materials are as follows [20]:

$$\boldsymbol{S} = \boldsymbol{s}^{\mathrm{e}}\boldsymbol{T} + \boldsymbol{dE} \tag{1}$$

$$\boldsymbol{D} = \boldsymbol{dT} + \boldsymbol{\varepsilon}^{\mathrm{t}}\boldsymbol{E} \tag{2}$$

where $\boldsymbol{S}$ and $\boldsymbol{T}$ are strain and stress tensors, respectively; $\boldsymbol{D}$ and $\boldsymbol{E}$ the electric displacement and electric field vectors, respectively; also, $\boldsymbol{s}^{\mathrm{e}}$ is the elastic compliance matrix evaluated in a constant electric field, $\boldsymbol{\varepsilon}^{\mathrm{t}}$ a matrix of permittivity values that are evaluated at a constant stress, and $\boldsymbol{d}$ a matrix of piezoelectric strain coefficients.

3. Theoretical Analysis of Energy Conversion

Based on the principle of the rainbow shape piezoelectric transducer, the generated electric energy depends on the deformation or stress distribution of the transducer. In the analysis, the theoretical derivation of the energy conversion efficiency is for quasi-static behavior and the excitation force applied to the rainbow shape piezoelectric transducer is F. Based on the calculation formulas of potential energy of piezoelectric materials and the mechanical analysis of the transducer, the generated charge and voltage of every piezoelectric film can be expressed as follows:

$$Q_i = \frac{E_\mathrm{p} R^2 d_{31} b_\mathrm{p}}{2h^2}\left[-\phi_{4,i} + (-1)^i \frac{1}{2}(t_\mathrm{p} + t_\mathrm{m})\phi_{5,i}\right] \quad (i=1,2) \tag{3}$$

$$V_i = \left\{\frac{E_\mathrm{p} R^2 d_{31} b_\mathrm{p}}{2h^2}\left[-\phi_{4,i} + (-1)^i \frac{1}{2}(t_\mathrm{p} + t_\mathrm{m})\phi_{5,i}\right]\right\} \Bigg/ \left\{\frac{E_\mathrm{p} R^2 d_{31}^2 b_\mathrm{p}^2 l_\mathrm{p}}{2h^2}\left[2\phi_{1,i} + \frac{1}{2}(t_\mathrm{p} + t_\mathrm{m})^2 \phi_{2,i} + (-1)^{i+1}(t_\mathrm{p} + t_\mathrm{m})\phi_{3,i}\right] + \frac{l_\mathrm{p}}{t_\mathrm{p}}(\varepsilon_{33} - d_{31}^2)\right\} \quad (i=1,2) \tag{4}$$

where $i=1$ denotes arc inside piezoelectric film and $i=2$ denotes arc outside piezoelectric film; E_p and E_m are the elastic modulus of the piezoelectric film and metal flexible substrate respectively; ε_{33} and d_{31} are the element of $\boldsymbol{\varepsilon}^{\mathrm{t}}$ and $\boldsymbol{d}$ respectively; and

$$h = c^2 - ae$$

$$a = 2E_\mathrm{p} b_\mathrm{p} t_\mathrm{p} + E_\mathrm{m} b_\mathrm{m} t_\mathrm{m}$$

$$c=\frac{1}{R}\left[E_{\rm p}b_{\rm p}t_{\rm p}\left(\frac{1}{2}t_{\rm m}^2+t_{\rm m}t_{\rm p}+\frac{2}{3}t_{\rm p}^2\right)+\frac{1}{12}E_{\rm m}b_{\rm m}t_{\rm m}^3\right]$$

$$e=RC$$

$$\phi_{1,i}=p_{1,i}e^2-2cep_{2,i}+p_{3,i}c^2$$

$$\phi_{2,i}=p_{1,i}c^2-2acp_{2,i}+p_{3,i}a^2$$

$$\phi_{3,i}=-2p_{1,i}ce+2p_{2,i}(c^2+ae)-2p_{3,i}ac$$

$$\phi_{4,i}=-2[p_{1,i}p_4e^2-p_{1,i}p_5ce-2p_{2,i}p_4ce+p_{2,i}p_5(c^2+ae)+p_{3,i}p_4c^2-p_{3,i}p_5ac]$$

$$\phi_{5,i}=-2[-p_{1,i}p_4ce+p_{1,i}p_5c^2+p_{2,i}p_4(c^2+ae)-2p_{2,i}p_5ac-p_{3,i}p_4ac+p_{3,i}p_5a^2]$$

$$p_{11}=\frac{4t_{\rm p}}{(2R-2t_{\rm p}-t_{\rm m})(2R-t_{\rm m})}$$

$$p_{21}=Rp_{11}+\ln\frac{2R-2t_{\rm p}-t_{\rm m}}{2R-t_{\rm m}}$$

$$p_{31}=t_{\rm p}-R^2p_{11}+2Rp_{21}$$

$$p_{12}=\frac{4t_{\rm p}}{(2R+2t_{\rm p}+t_{\rm m})(2R+t_{\rm m})}$$

$$p_{22}=Rp_{12}+\ln\frac{2R+t_{\rm m}}{2R+t_{\rm m}+2t_{\rm p}}$$

$$p_{32}=t_{\rm p}-R^2p_{12}+2Rp_{22}$$

$$p_4=-2FR\sin\left(l_{\rm p}/2R\right)$$

$$p_5=FR[l_{\rm p}\cos(l_{\rm m}/2R)-2R\sin(l_{\rm p}/2R)]$$

Based on Eqs. (3)-(4), the potential energy under constant voltage and constant current can be deduced. For the short circuit, there will be V_i=0, which is equivalent to constant voltage.

For the flexible substrate, the potential energy density can be described as

$$\mathrm{d}u_{\rm m}=\frac{1}{2}S_{1,\rm m}T_{1,\rm m}=\frac{1}{2}E_{\rm m}S_{1,\rm m}^2 \tag{5}$$

where $\mathrm{d}u_{\rm m}$, $S_{1,\rm m}$ and $T_{1,\rm m}$ are the potential energy density, the strain and the stress of the flexible substrate, respectively.

Thus, the constant voltage potential energy of the flexible substrate is

$$U_{\rm m}^V=\int_{v_3}\mathrm{d}u_{\rm m}^V\mathrm{d}v_3=\iiint_{v_3}\mathrm{d}u_{\rm m}^V\mathrm{d}x\mathrm{d}y\mathrm{d}z \tag{6}$$

By Eq. (6), the constant voltage potential energy of the flexible substrate can be obtained as follows:

$$U_{\rm m}^V=\frac{E_{\rm m}R^2}{2h^2}[b_{\rm m}p_{13}(p_{63}e^2+p_{73}c^2-2p_{83}ce)+b_{\rm m}p_{33}(p_{63}c^2+p_{73}a^2-2p_{83}ac)+b_{\rm m}p_{23}(-2p_{63}ce+2p_{83}ae+2p_{83}c^2-2p_{73}ac)] \tag{7}$$

where

$$p_{13}=\frac{4t_{\rm m}}{(2R-t_{\rm m})(2R+t_{\rm m})}$$

$$p_{23}=\ln\frac{2R-t_{\rm m}}{2R+t_{\rm m}}+\frac{4t_{\rm m}R}{(2R-t_{\rm m})(2R+t_{\rm m})}$$

$$p_{33}=t_{\rm m}-R^2p_{13}+2Rp_{23}$$

$$p_{63}=F^2R\left(\frac{l_{\rm m}}{2R}+\frac{1}{2}\sin\frac{l_{\rm m}}{R}\right)$$

$$p_{73}=F^2R^2\left[l_{\rm m}\cos^2\frac{l_{\rm m}}{2R}-4R\cos\frac{l_{\rm m}}{2R}\cdot\sin\frac{l_{\rm m}}{2R}+R\left(\frac{l_{\rm m}}{2R}+\frac{1}{2}\sin\frac{l_{\rm m}}{2R}\right)\right]$$

$$p_{83}=-F^2R^2\left(\frac{1}{2}\sin\frac{l_{\rm m}}{R}-\frac{l_{\rm m}}{2R}\right)$$

For the piezoelectric film, the potential energy density can be described as

$$\mathrm{d}u_{\rm p}=\frac{1}{2}S_{1,\rm p}T_{1,\rm p}+\frac{1}{2}D_3E_3=\frac{1}{2}E_{\rm p}S_{1,\rm p}^2-\frac{1}{2}E_{\rm p}d_{31}^2E_3^2+\frac{1}{2}\varepsilon_{33}E_3^2 \tag{8}$$

where $\mathrm{d}u_{\rm p}$, $S_{1,\rm p}$ and $T_{1,\rm p}$ are the potential energy density, strain and stress of the piezoelectric film, and D_3 and E_3 the electric displacement and the electric field of the piezoelectric film.

Correspondingly, the constant voltage potential energy of the inside piezoelectric film of the rainbow shape piezoelectric transducer is

$$U_{\rm p1}^V=\int_{v_1}\mathrm{d}u_{\rm p1}^V\mathrm{d}v_1=\iiint_{v_1}\mathrm{d}u_{\rm p1}^V\mathrm{d}x\mathrm{d}y\mathrm{d}z \tag{9}$$

By Eq. (9), the constant voltage potential energy of the inside piezoelectric film of the rainbow shape piezoelectric transducer can be obtained as follows:

$$U_{\rm p1}^V=\frac{E_{\rm p}R^2}{2h^2}[b_{\rm p}p_{11}(p_6e^2+p_7c^2-2p_8ce)+b_{\rm p}p_{31}(p_6c^2+p_7a^2-2p_8ac)+b_{\rm p}p_{21}(-2p_6ce+2p_8ae+2p_8c^2-2p_7ac)] \tag{10}$$

where

$$p_6=F^2R\left(\frac{l_{\rm p}}{2R}+\frac{1}{2}\sin\frac{l_{\rm p}}{R}\right)$$

$$p_7=F^2R^2\left[l_{\rm p}\cos^2\frac{l_{\rm m}}{2R}-4R\cos\frac{l_{\rm m}}{R}\cdot\sin\frac{l_{\rm p}}{2R}+R\left(\frac{l_{\rm p}}{2R}+\frac{1}{2}\sin\frac{l_{\rm p}}{R}\right)\right]$$

$$p_8=-F^2R^2\left(2\sin\frac{l_{\rm p}}{2R}\cos\frac{l_{\rm m}}{2R}-\frac{1}{2}\sin\frac{l_{\rm p}}{R}-\frac{l_{\rm p}}{2R}\right)$$

The constant voltage potential energy of the outside piezoelectric film of the rainbow shape piezoelectric transducer is

$$U_{\mathrm{p2}}^{V}=\int_{v_2}\mathrm{d}u_{\mathrm{p2}}^{V}\mathrm{d}v_2=\iiint_{v_2}\mathrm{d}u_{\mathrm{p2}}^{V}\mathrm{d}x\mathrm{d}y\mathrm{d}z \tag{11}$$

Based on Eq. (11), the constant voltage potential energy of the outside piezoelectric film of the rainbow shape piezoelectric transducer can be obtained as follows:

$$U_{\mathrm{p2}}^{V}=\frac{E_{\mathrm{p}}R^2}{2h^2}[b_{\mathrm{p}}p_{12}(p_6e^2+p_7c^2-2p_8ce)+ b_{\mathrm{p}}p_{32}(p_6c^2+p_7a^2-2p_8ac)+b_{\mathrm{p}}p_{22}\cdot (-2p_6ce+2p_8ae+2p_8c^2-2p_7ac_4)] \tag{12}$$

By Eq. (7), Eq. (10) and Eq. (12), the total potential energy of the whole rainbow shape piezoelectric transducer in the case of constant voltage can be written as

$$U^V=U_{\mathrm{m}}^{V}+U_{\mathrm{p1}}^{V}+U_{\mathrm{p2}}^{V} \tag{13}$$

For the open circuit, both the current and the applied external voltage are zero. Thus, the voltage on the rainbow shape piezoelectric transducer is equivalent to the generated voltage V_i. According to Eq. (5), the constant current potential energy of the flexible substrate can be obtained:

$$U_{\mathrm{m}}^{I}=\frac{E_{\mathrm{m}}R^2}{2h^2}\left(b_{\mathrm{m}}p_{13}\psi_{1,\mathrm{m}}+b_{\mathrm{m}}p_{33}\psi_{2,\mathrm{m}}+b_{\mathrm{m}}p_{23}\psi_{3,\mathrm{m}}\right) \tag{14}$$

where

$$p_{43}=-2FR\sin(l_{\mathrm{m}}/2R)$$
$$p_{53}=F[l_{\mathrm{m}}\cos(l_{\mathrm{m}}/2R)-2R\sin(l_{\mathrm{m}}/2R)]$$
$$\psi_{1,\mathrm{m}}=p_{63}e^2+p_{73}c^2+l_{\mathrm{m}}J_1^2e^2+l_{\mathrm{m}}J_2^2c^2- 2p_{83}ce-2p_{43}J_1e^2+2p_{43}J_2ce+ 2p_{53}J_1ce-2p_{53}J_2c^2-2l_{\mathrm{m}}J_1J_2ce$$
$$\psi_{2,\mathrm{m}}=p_{63}c^2+p_{73}a^2+l_{\mathrm{m}}J_1^2c^2+l_{\mathrm{m}}J_2^2a^2- 2p_{83}ac-2p_{43}J_1c^2+2p_{43}J_2ac+ 2p_{53}J_1ac-2p_{53}J_2a^2-2l_{\mathrm{m}}J_1J_2ac$$
$$\psi_{3,\mathrm{m}}=-2p_{63}ce-2p_{73}ac-2l_{\mathrm{m}}J_1^2ce+ 2l_{\mathrm{m}}J_1J_2ae-2l_{\mathrm{m}}J_2^2ac+2p_{83}ae+ 2p_{83}c^2+4p_{43}J_1ce-2p_{43}J_2ae- 2p_{43}J_2c^2-2p_{53}J_1c^2+4p_{53}J_2ac- 2p_{53}J_1ae+2l_{\mathrm{m}}J_1J_2c^2$$
$$J_1=-E_{\mathrm{p}}d_{31}b_{\mathrm{p}}(V_1+V_2)$$
$$J_2=0.5E_{\mathrm{p}}d_{31}b_{\mathrm{p}}(t_{\mathrm{p}}+t_{\mathrm{m}})(V_2-V_1)$$

According to Eq. (8), the constant current potential energy of the inside piezoelectric film of the rainbow shape piezoelectric transducer can be obtained:

$$U_{\mathrm{p1}}^{I}=\frac{E_{\mathrm{p}}R^2}{2h^2}(b_{\mathrm{p}}p_{11}\psi_{1,\mathrm{p}}+b_{\mathrm{p}}p_{31}\psi_{2,\mathrm{p}}+b_{\mathrm{p}}p_{21}\psi_{3,\mathrm{p}})- (0.5E_{\mathrm{p}}d_{31}^2V_1^2l_{\mathrm{p}}b_{\mathrm{p}})/t_{\mathrm{p}}+(0.5\varepsilon_{33}V_1^2l_{\mathrm{p}}b_{\mathrm{p}})/t_{\mathrm{p}} \tag{15}$$

where

$$\psi_{1,\mathrm{p}}=p_6e^2+p_7c^2+l_{\mathrm{p}}J_1^2e^2+l_{\mathrm{p}}J_2^2c^2- 2p_8ce-2p_4J_1e^2+2p_4J_2ce+ 2p_5J_1ce-2p_5J_2c^2-2l_{\mathrm{p}}J_1J_2ce$$
$$\psi_{2,\mathrm{p}}=p_6c^2+p_7a^2+l_{\mathrm{p}}J_1^2c^2+l_{\mathrm{p}}J_2^2a^2- 2p_8ac-2p_4J_1c^2+2p_4J_2ac+ 2p_5J_1ac-2p_5J_2a^2-2l_{\mathrm{p}}J_1J_2ac$$
$$\psi_{3,\mathrm{p}}=-2p_6ce-2p_7ac-2l_{\mathrm{p}}J_1^2ce+ 2l_{\mathrm{p}}J_1J_2ae-2l_{\mathrm{p}}J_2^2ac+2p_8ae+2p_8c^2+ 4p_4J_1ce-2p_4J_2ae-2p_4J_2c^2-2p_5J_1c^2+ 4p_5J_2ac-2p_5J_1ae+2l_{\mathrm{p}}J_1J_2c^2$$

Correspondingly, the constant current potential energy of the outside piezoelectric film of the rainbow shape piezoelectric transducer is

$$U_{\mathrm{p2}}^{I}=\frac{E_{\mathrm{p}}R^2}{2h^2}[b_{\mathrm{p}}p_{12}\psi_{1,\mathrm{p}}+b_{\mathrm{p}}p_{32}\psi_{2,\mathrm{p}}+b_{\mathrm{p}}p_{22}\psi_{3,\mathrm{p}}]- (0.5E_{\mathrm{p}}d_{31}^2V_2^2l_{\mathrm{p}}b_{\mathrm{p}})/t_{\mathrm{p}}+(0.5\varepsilon_{33}V_2^2l_{\mathrm{p}}b_{\mathrm{p}})/t_{\mathrm{p}} \tag{16}$$

By Eqs. (14)-(16), the total potential energy of the whole rainbow shape piezoelectric transducer in the case of constant current can be written as

$$U^I=U_{\mathrm{m}}^{I}+U_{\mathrm{p1}}^{I}+U_{\mathrm{p2}}^{I} \tag{17}$$

According to the definition of the effective electromechanical coupling coefficient, the effective electromechanical coupling coefficient of the rainbow shape piezoelectric transducer can be expressed as

$$k_{\mathrm{eff}}^2=1-\frac{U^V}{U^I} \tag{18}$$

By substitution of Eq. (13) and Eq. (17) into Eq. (18), then the effective electromechanical coupling coefficient can be obtained.

As the effective electromechanical coupling coefficient is calculated out, then the maximal energy conversion efficiency can be obtained as follows:

$$\eta_{\max}=\frac{k_{\mathrm{eff}}^2}{4-2k_{\mathrm{eff}}^2} \tag{19}$$

4. Simulation and Analysis

4.1. Comparison of generated voltage with data from finite element simulation and experiment

The performance of the rainbow shape piezoelectric transducer can be obtained by the analytical equation derived above. However, the analytical equation needs to be verified because of some assumptions applied during the derivation. One effective method to verify the analytical equation is to compare the analytical results with the finite element (FE) results and experimental results. Here, only the generated voltage of the rainbow shape piezoelectric transducer with beryllium bronze substrate is considered. In the calculations, we use polyvinylidene fluoride (PVDF) as the piezoelectric material and use beryllium bronze as the flexible substrate material. Furthermore, the solid-98 is chosen to model the piezoelectric layer and the solid-92 is used to model the flexible substrate. Table 1 gives the material properties and structural parameters of the rainbow shape piezoelectric transducer analyzed in this paper. The other parameters of the transducer are given as

$$\boldsymbol{e} = \begin{bmatrix} 0 & 0 & 0.010\,4 \\ 0 & 0 & -0.016\,4 \\ 0 & 0 & -0.065\,0 \\ 0 & 0 & 0 \\ -0.038\,8 & 0 & 0 \\ 0 & 0 & 0 \end{bmatrix}$$

$$\boldsymbol{c} = \begin{bmatrix} 8.10 & 4.84 & 4.84 & 0 & 0 & 0 \\ 4.84 & 6.92 & 4.38 & 0 & 0 & 0 \\ 4.84 & 4.38 & 6.92 & 0 & 0 & 0 \\ 0 & 0 & 0 & 1.38 & 0 & 0 \\ 0 & 0 & 0 & 0 & 1.38 & 0 \\ 0 & 0 & 0 & 0 & 0 & 1.38 \end{bmatrix}$$

where the unit of $\boldsymbol{e}$ is C/m^2 and the unit of $\boldsymbol{c}$ is 10^9 N/m^2.

Table 1 Dimensions and material properties of rainbow shape piezoelectric transducer

Parameter	PVDF	Berylium bronze	Steel
Density/(kg·m^{-3})	1 780	8 290	7 800
Elastic modulus/GPa		131	210
Poisson ratio	0.3	0.35	0.3
Thickness/mm	0.2	0.1	0.1
Width/mm	4	4	4
Length/mm	12	12	12
Relative dielectric constant	12		
Initial curvature radius/mm		8	

Figure 2 shows the relationship between analytical solution, FE simulation and experiment results generated by voltages and the piezoelectric film thickness when a constant excitation force 1.0 N is applied. The optimal thicknesses of the piezoelectric film from the analytical solution, FE simulation and experiment are all 0.2 mm. It can be found that the results from analytical solution are in a good agreement with the FE simulation results and experimental results. This suggests that the derived analytical equations are valid.

4.2. *Energy conversion efficiency*

In order to demonstrate the influence of shape parameters and materials of the rainbow shape piezo electric transducer on energy conversion efficiency,

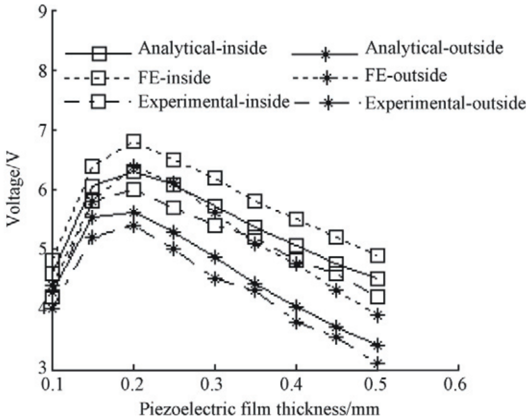

Fig. 2 Effect of piezoelectric film thickness on generated voltage.

some numerical results are presented in the following text.

Here, the length ratio of the piezoelectric film to flexible substrate is denoted by $\alpha = l_p/l_m$. Figure 3 shows the effect of the length ratio on energy conversion efficiency of the rainbow shape piezoelectric transducer with beryllium bronze flexible substrate and steel flexible substrate under constant external force 1.0 N. Obviously, the optimal length ratios of the rainbow shape piezoelectric transducer with beryllium bronze flexible substrate and steel flexible substrate are both 0.65, and the maximum energy conversion efficiencies of the transducers are 2.21% and 1.64% respectively.

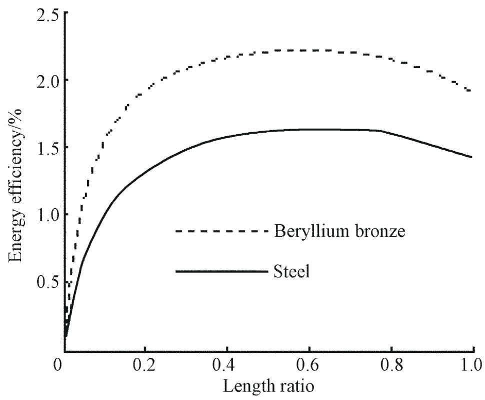

Fig. 3 Effect of length ratio on energy efficiency.

The thickness ratio of the piezoelectric film to flexible substrate is denoted by $\beta = t_p/t_m$. Figure 4 presents the relationships between the energy conversion efficiencies and thickness ratios of the two transducers under constant external force 1.0 N. It can be found that the optimal thickness ratios for the transducers to obtain peak energy conversion efficiencies are different and the optimal thickness ratios of the transducers with beryllium bronze flexible substrate and steel flexible substrate are 1.16 and 1.49 respectively. Correspondingly, the maximum energy conversion efficiencies of the transducers are 2.56% and 1.57% respectively.

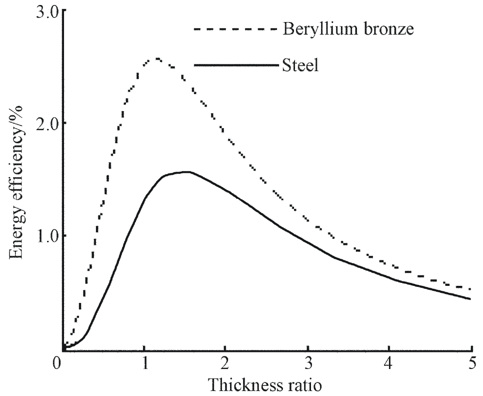

Fig. 4 Effect of thickness ratio on energy efficiency.

Comparing Fig. 3 with Fig. 2, it is found that the optimal thickness ratios for the beryllium bronze substrate transducer to obtain maximal voltage and maximal energy conversion efficiency are different. The reason is that the energy conversion efficiency depends on the converted electric energy and the converted electric energy is the product of voltage and charge. Furthermore, the charge decreases with the increase of thickness ratio. Therefore, the optimal thickness ratio for energy conversion efficiency is smaller than that for voltage.

Furthermore, the simulation results suggest that the transducer with optimal length ratio and thickness ratio has the largest energy conversion efficiency. The reason is that the converted electric energy of the transducer increases with the increase of the length ratio, whereas the strain of the transducer decreases. As a result, the energy conversion efficiency of the transducer would reach maximum at an optimal length ratio. As the thickness ratio changes, the results of the energy conversion efficiency are similar to the length ratio.

The width ratio of the piezoelectric film to flexible substrate is denoted by $\gamma = b_m / b_p$. Figures 5-6 show the effect of the width ratio and initial curvature radius on energy conversion efficiency of the rainbow shape piezoelectric transducer under constant external force 1.0 N. It can be found that the energy conversion efficiencies of the transducers both decrease as the width ratio and initial curvature radius increase. However, the effect of the initial curvature radius is smaller. This suggests that the transducers with smaller width ratio and initial curvature radius have larger energy conversion efficiency. The reason is that the strain of the transducer decreases as the width ratio increases, so small width ratio will be beneficial for converting electric energy. In addition, the normal component of the exciting force decreases with the increase of the initial curvature radius. As a result, the strain of the transducer decreases.

Furthermore, it can be found that the energy conversion efficiency of the transducer with beryllium bronze flexible substrate is larger than that of steel flexible substrate. It suggests that beryllium bronze flexible substrate transducer is superior to the steel substrate transducer and the beryllium bronze should be utilized for the rainbow shape piezoelectric transducer to enhance the energy conversion efficiency.

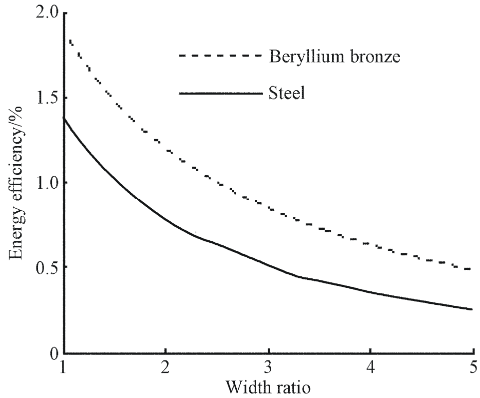

Fig. 5 Effect of width ratio on energy efficiency.

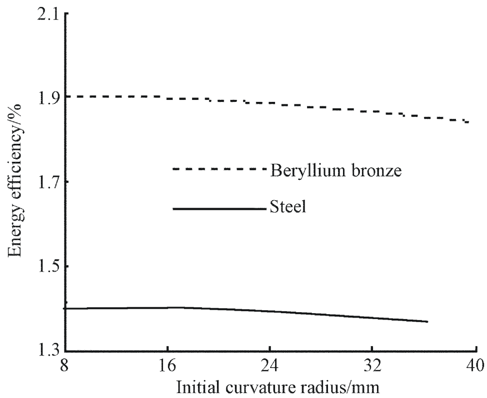

Fig. 6 Effect of initial curvature radius on energy efficiency.

5. Conclusions

A method is presented to estimate the energy conversion efficiency of the rainbow shape piezoelectric transducer. The research results show that both the shape parameters and elastic modulus exert great influence on energy conversion efficiency and the results obtained from analytical equation are in a good agreement with those from FE results and experimental results. With the increase of length ratio, there is an optimal length ratio to generate maximum energy conversion efficiency, and the optimal length ratios and energy conversion efficiencies of beryllium bronze substrate transducer and steel substrate transducer are (0.65, 2.21%) and (0.65, 1.64%) respectively. The optimal thickness ratios and energy conversion efficiencies of beryllium bronze substrate transducer and steel substrate transducer are (1.16, 2.56%) and (1.49, 1.57%) respectively. With the increases of width ratio and initial curvature radius, the energy conversion efficiencies both decrease. On the other hand, beryllium bronze flexible substrate transducer is superior to the steel flexible substrate transducer. Although the theoretical derivation of the energy conversion efficiency is quasi-static behavior and it is not directly applicable for vibration-based energy harvesting, it is helpful for the optimization design of the rainbow shape piezoelectric transducer.

References

[1] Roundy S, Wright P K, Pister K S. Micro-electrostatic vibration to electricity converters. Proceedings of ASME International Mechanical Engineering Congress & Exposition. New Orleans, Louisiana: ASME, 2002: 1-10.

[2] Roundy S, Write P K, Rabaey J. A study of low level vibrations as a power source for wireless sensor nodes. Computer Communications 2003; 26(11): 1131-1144.

[3] Roundy S, Write P K. A piezoelectric vibration based generator for wireless electronics. Smart Materials and Structures 2004; 13(5): 1131-1142.

[4] Shen D, Park J H, Ajitsaria J, et al. The design, fabrication and evaluation a MEMS PZT cantilever with an integrated Si proof mass for vibration energy harvesting. Journal of Micromechanics and Microengineering 2008; 18(5): 550-557.

[5] Chew Z J, Li L J. Design and characterization of a piezoelectric scavenging device with multiple resonant frequencies. Sensors and Actuators: A 2010; 162(1): 82-92.

[6] Liu J Q, Fang H B, Xu Z Y, et al. A MEMS-based piezoelectric power generator array for vibration energy harvesting. Microelectronics 2008; 39(5): 802-806.

[7] Erturk A, Renno J M, Inman D J. Piezoelectric energy harvesting from a L-shaped beam-mass structure with an application to UAVs. Journal of Intelligent Material Systems and Structures 2009; 20(5): 529-544.

[8] Jeong S J, Kim M S, Song J S. Two-layered piezoelectric bender device for micro-power generator. Sensors and Actuators: A 2008; 148(1): 158-167.

[9] Guan M J, Liao W H. On the efficiencies of piezoelectric energy harvesting circuits towards storage device voltages. Smart Materials and Structures 2007; 16(2): 498-505.

[10] Xue H, Hu Y T, Wang Q M. Broadband piezoelectric energy harvesting devices using multiple bimorphs with different operating frequencies. IEEE Transactions on Ultrasonics Ferroelectrics and Frequency Control 2008; 55(9): 2104-2108.

[11] Ingo K, Djordje M, Gerald E. A new approach for MEMS power generation based on a piezoelectric diaphragm. Sensors and Actuators: A 2008; 142(1): 292-297.

[12] Feenstra J, Granstrom J, Sodano H. Energy harvesting through a backpack employing a mechanically amplified piezoelectric stack. Mechanical Systems and Signal Processing 2008; 22(3): 721-734.

[13] Liao Y, Sodano H A. Structural effects and energy conversion efficiency of power harvesting. Journal of Intelligent Material Systems and Structures 2009; 20(5): 505-514.

[14] Mitcheson P D, Miao P, Stark B H, et al. MEMS electrostatic micropower generator for low frequency operation. Sensors and Actuators: A 2004; 115(2-3): 523-529.

[15] Wang P H, Dai X H, Fang D M, et al. Design, fabrication and performance of a new vibration-based electromagnetic micro power generator. Microelectronics 2007; 38(12): 1175-1180.

[16] Kim H, Priya S, Uchino K. Modeling of piezoelectric energy harvesting using cymbal transducers. Japanese Journal of Applied Physics 2006; 45(7): 5836-5840.

[17] Wang S, Lam K H, Sun C L, et al. Energy harvesting with piezoelectric drum transducer. Applied Physics Letters 2007; 90(11): 1135061-1135063.

[18] Priya S, Chen C T, Fye D, et al. Piezoelectric windmill: a novel solution to remote sensing. Japanese Journal of Applied Physics 2005; 44(3): 104-107.

[19] Liu X J, Chen R W. Analysis of the load voltage and output power for rainbow shape piezoelectric monomorph energy transferring elements. Acta Aeronautica et Astronautica Sinica 2011; 32(3): 561-570. [in Chinese]

[20] Jiang S N, Li X F, Guo S H, et al. Performance of a piezoelectric bimorph for scavenging vibration energy. Smart Materials and Structures 2005; 14(5): 769-774.

Biographies:

LIU Xiangjian is a Ph.D. candidate of Nanjing University of Aeronautics and Astronautics. His main research interest lies in vibration energy harvesting.
E-mail: liuxukd@126.com

CHEN Renwen is a professor with Ph.D. degree of Nanjing University of Aeronautics and Astronautics. His main research interest is smart materials and structures.
E-mail: rwchen@nuaa.edu.cn

ZHU Liya is a Ph.D. candidate of Nanjing University of Aeronautics and Astronautics. Her main research interest is vibration energy harvesting.
E-mail: julia_860527@163.com